

Tse-Shien Chen
Chuen-Ying Liu

Department of Chemistry,
National Taiwan University,
Taipei, Taiwan

Histidine-functionalized silica and its copper complex as stationary phases for capillary electrochromatography

A histidine-functionalized silica was prepared by covalent bonding of the functional groups to silane-treated silica gel. Conversion of functional groups was confirmed by infrared (IR) spectra, elemental analysis, and potentiometry. The functionality of the silica gel is $0.293 \text{ mmol g}^{-1}$. The coordination behavior of the histidine-functionalized silica was investigated by metal capacity and electron paramagnetic resonance (EPR). EPR measurements at different copper loadings were made. The results showed that the copper histidine complex might be distorted tetragonal. Both histidine-functionalized silica and its copper complex were employed as stationary phases for packed capillary electrochromatography (CEC). Electrical current was found helpful for evaluating the properties of frit construction and the stationary phase packing. Test samples include neutral compounds, inorganic anions and organic anions. Factors influencing the separation behavior have been studied. With copper-histidine functionalized silica under the condition of citrate buffer (10 mM, pH 4.0) and applied voltage of -20 kV , the separation of benzoic acid, D- and L-mandelic acid, phthalic acid and salicylic acid could be achieved within 12 min. The column efficiency for these acids was more than $1.2 \times 10^5 \text{ plates m}^{-1}$, except salicylic acid.

Keywords: Histidine-functionalized silica / Copper-histidine functionalized silica complex / Capillary electrochromatography / Stationary phase
EL 4501

1 Introduction

Capillary electrochromatography (CEC) can be viewed as a hybrid between capillary electrophoresis (CE) and microcolumn (capillary) liquid chromatography (μLC): its separation mechanism is largely chromatographic, while the mobile-phase transport is mediated by the electroosmotic action [1]. Despite the many advantages of CEC that have been demonstrated, several technical problems have slowed the development and general acceptance of CEC [2]. These include making suitable frits and packing stationary phases into a column. Likewise, packing very long columns would be a difficult task. Therefore, the main focus of future research will be on solving current problems and improving the column technology [3–7].

The driving force in CEC is the electroosmotic flow (EOF) and this is highly dependent on pH, the buffer concentration, the organic modifier, and the type of stationary phase. The chemistry used to prepare the stationary phase can have a dramatic effect not only on the separa-

tion but also on the speed of analysis. The vast majority of examples of CEC to date have been performed on either C_8 or C_{18} stationary phases and this is not surprising considering the prolific amount of data available on these phases from the HPLC literature, while the other modes are much farther behind. The possibility of using different HPLC stationary phases is often viewed as “higher selectivity” for CEC.

Several ion-exchange stationary phases have been introduced into CEC for the analysis of charged organic solutes [8–11], inorganic ions [12] or chiral analytes [13, 14]. Voltage-induced sample release from anion-exchange supports in CEC was studied by Kitagawa and Tsuda [15]. Specially developed packings for CEC in which silica particles were coated with a mixture of sulfonic acid groups or amino groups and alkyl moieties have been reported [16–18]. The alkyl chains act as stationary phases to retain solutes while the charged groups result in high EOF at low pH. The retention behavior of glycosphingolipids on the octadecyl-sulfonated silica was also investigated by Zhang *et al.* [19]. Spikmans *et al.* [20] used a Hypersil Duet C_{18} /strong cation exchanger (SCX) mixed-mode column for the separation of corticosteroids. Ye *et al.* [21] used a strong cation-exchange packing based on silica as the stationary phase and dynamically modified by CTAB for the performance of CEC. The separation of neutral, acidic, and basic compounds

Correspondence: Professor Chuen-Ying Liu, Department of Chemistry, National Taiwan University, Taipei 10617, Taiwan
E-mail: cylieu@ccms.ntu.edu.tw
Fax: +886-2-23638543

Abbreviations: EPR, electron paramagnetic resonance; IR, infrared; ODS, octadecyl silica

was investigated. Mix-mode stationary phase (C_6 /strong anion (SAX)) has also been employed as a means for the simultaneous separation of acidic, basic and neutral compounds in a single CEC run by Haddad and co-workers [22]. Several mechanisms including electrophoretic migration, ion-exchange and hydrophobic interaction are involved in the separation of the test solutes.

Histidine (pI 7.6) as functional group of chelating ion exchangers has been used for soft metal ion extraction [23], metal ion elution from a chelating stationary phase [24], a dipolar eluent component in cation chromatography [25], and mobile phase of electrostatic ion chromatography [26]. In this paper, we describe the preparation of a histidine-functionalized silica and its copper complex as the stationary phases for CEC. At pH values below the pI , histidine would behave with cationic properties and act as an anion exchanger. Its metal complex could be employed as the ligand exchange property for the separation of electron-donating compounds. Meanwhile, the correlation between the construction of column packing, frit formation, and electrical current has also been discussed.

2 Materials and methods

2.1 Chemicals and materials

Fused-silica (100 μm ID) capillaries were purchased from Resteck (Bellefonte, PA, USA). Most chemicals were analytical reagent grade from Merck (Darmstadt, Germany). Purified water (18 $M\Omega$ -cm) from a Milli-Q water purification system (Millipore, Bedford, MA, USA) was used to prepare solutions. All solvents and solutions for CEC analysis were filtered through a 0.45 μm PTFE membrane (Millipore) and degassed prior to use. Silica gel (40 ~ 60 mesh and Superspher Si60, 5 μm), sodium chloride, sodium dihydrogen phosphate, potassium biphthalate, sodium nitrate, sodium nitrite, sodium sulfate, citric acid, benzoic acid, mandelic acid, sodium acetate, sodium hydroxide, and ethylenediaminetetraacetic acid (Merck, Darmstadt, Germany), salicylic acid, benzyl alcohol and thiourea (Wako, Japan), 3-chloropropyltrimethoxysilane and sodium silicate (Aldrich, Milwaukee, WI, USA), *m*-xylene (Janssen, Belgium), histidine and dimethyl sulfoxide (Sigma, St. Louis, MO, USA), benzene and mesityl oxide (Acros, Geel, Belgium) were purchased from the indicated sources. All liquid reagents and solvents used in moisture-sensitive reactions were distilled and collected over type 4 Å molecular sieves.

2.2 Synthetic procedure

In this study, two kinds of commercial silica gel support were employed. For the characterization, silica gel (40–60 mesh, 20 g) was ground and sieved to give a particle size of 3–5 μm with Octagon 200 and Sonic Sifter (Endecotts, UK). For analytical application in CEC, silica gel (Superspher Si60, 5 μm) was used. After being washed with pure water, the silica gel was refluxed under isopropanol for 2 h to remove organic impurities. The reactant mixture was then filtered and washed with acetone and pure water sequentially. The material was then ready for use. For preparation of histidine-functionalized silica, the purified silica gel (10 g) and dimethyl sulfoxide (DMSO) (100 mL) were placed in a round bottomed flask (100 mL) with efficient stirring at 140°C and refluxed for 12 h, to make the silica gel swell fully. Then 3-chlorotrimethoxypropylsilane (3 g) was added dropwise to the reaction mixture and further refluxed for 8 h. After the colorless DMSO turned to pale yellow, histidine (1 g) was added and the resultant mixture was reacted at 160°C, till the color of the silica gel turned dark-brown. The reactant mixture was poured into pure water (300 mL) to remove unreacted histidine. Then it was filtered and washed with water and acetone sequentially. The air-dried product was ready for use.

2.3 Characterization

The composition and structure of the product at each step in the synthesis were characterized by elemental analysis and IR spectra. The functionalities of histidine on silica gel were estimated from the nitrogen content. The copper capacities as a function of pH were measured. The dissociation constant of the histidine-functionalized silica was determined potentiometrically in a solution of 0.1 M ionic strength in KCl. To 50 mL of this solution 0.1 g of histidine-functionalized silica was added.

2.4 Column preparation

CEC columns with histidine-functionalized silica or its copper complex were packed in-house by a slurry-packing technique. Each capillary column was flushed first with 1 M NaOH (10 min), 0.1 M NaOH (5 min), then with pure water (10 min), 1 M HCl (10 min) and pure water (10 min) sequentially.

2.5 Preparation of packed column for CEC

Most of the procedures were modified from those of Cikalo [11]. Sections of capillaries (typically 40 cm length) were packed using a Chemco HPLC column packer

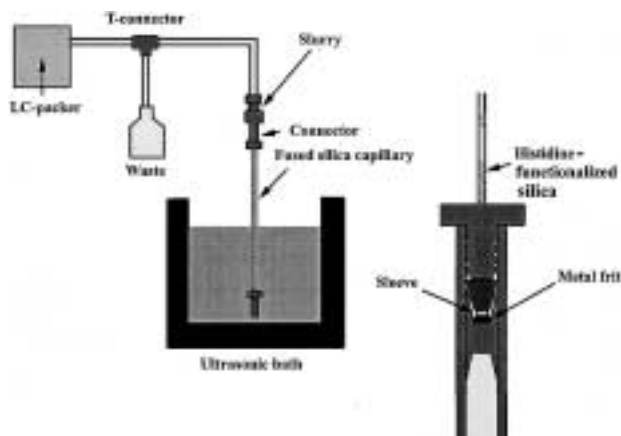


Figure 1. Packing device for the CEC packed column.

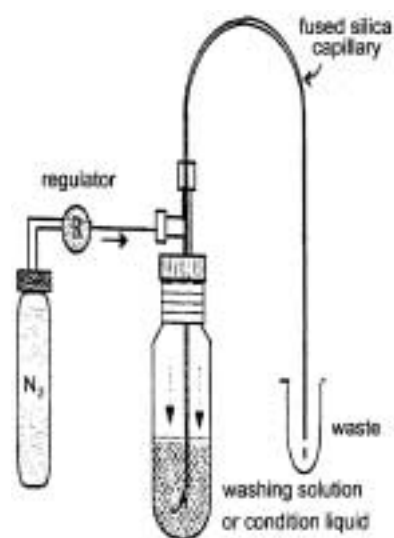


Figure 2. Low-pressure capillary rising device for column preconditioning.

(EchonoPacker CPP-085, Japan) equipped with an air compressor operating at 600 kg/cm². The reservoir, containing slurry of the stationary phase in acetone, was sonicated throughout, and methanol was used as the packing solvent. The capillary was typically packed within the first few minutes, after which the pressure was maintained at 400 kg/cm² for a further 1 h to ensure a firmly packed bed. During the packing, the end of the fused-silica capillary was connected to a Valco union with a metal screen (0.5 μm pores) to prevent the material being expelled from the capillary. The packing device is shown as Fig. 1. Frit preparation was according to Yamamoto's method [27]. CEC columns were conditioned from storage by a low pressure capillary rising device (Fig. 2) with the relevant electrolyte and they were then installed in the instrument for voltage conditioning until a steady current

was obtained. CEC experiments were performed with capillaries of total length around 78 cm. The separations were carried out on coupled capillaries connected *via* a PTFE sleeve.

2.6 CEC

The CEC experiments were performed with a Spectra-PHORESIS 100 electrophoresis system (Thermo Separation Products, Fremont, CA, USA) equipped with an UV absorbance detector (Spectra Focus Scanning CE detector) using PC 1000 software V. 3.0 for system control, data acquisition and data analysis. There is no pressure applied to the packed column in this system. Once the packed column was installed, it was further conditioned by driving the mobile phase through the capillary at an applied voltage of -5 kV for 1 h prior to use. Samples were introduced electrokinetically at the cathodic end of the capillary column. The appropriate mobile phase employed for the organic acid separations was citrate buffer. Separations were performed at an applied voltage of -20 kV. The analytes were detected by monitoring their absorbance at 220 nm.

3 Results and discussion

3.1 Characterization

The histidine-functionalized silica was characterized by elemental analysis, IR spectrum, hydrogen capacity and metal capacity. The detailed procedures were carried out according to [28]. The functionality was 0.293 mmol g⁻¹. The titration curve was shown as Fig. 3. This is a heterogeneous system; the equilibrium cannot be attained as fast as in a homogeneous system. Hence the titration could not be carried out continuously in a single vessel. Accordingly a small amount and higher concentration of NaOH (2 μL, 0.2 M) each time was added to a large volume of aqueous solution (50 mL) containing the histidine-functionalized silica (0.1 g). From the titration curve the estimated pK_a value is 2.8 for the carboxyl group and 8.0 for the protonated imidazole nitrogen. By comparison with the pK_a values of the histidine monomer (1.9 for the carboxyl group, 6.1 for the imidazole nitrogen), the results are reasonable since the silica gel support has a steric hindrance for the bonded functional groups.

The copper capacities of the histidine-functionalized silica at various pH values were studied (Table 1). The results show that the metal capacity at pH 5.0 is 0.15 mmol g⁻¹. Compared with the functionality of the prepared silica, a 1:2 metal ligand ratio was indicated. Electron paramagnetic resonance (EPR) studies of copper complexes yield valuable information regarding the

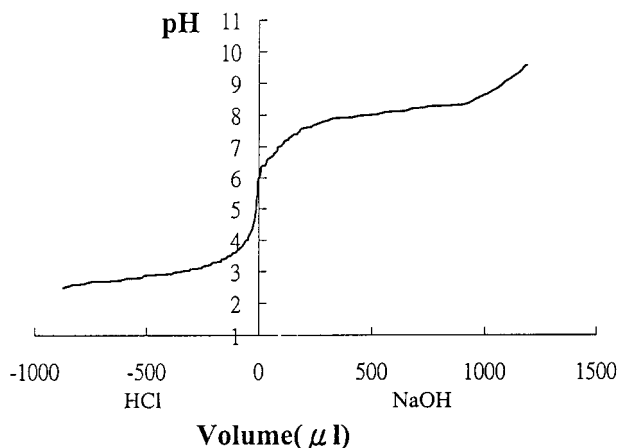


Figure 3. Titration curve of the histidine-functionalized silica. Histidine-functionalized silica, 0.1 g; volume of solution, 50 mL; ionic strength, 0.1 M KCl; titrant, 2 μ L NaOH (0.2 M) or HCl (0.2 M) for each increment.

Table 1. Parameters of the EPR spectra for histidine functionalized silica-copper complexes

pH	Capacity (mmol g ⁻¹)	g_{\perp}	g_{\parallel}	A(G)	$G^a)$	$\Delta H_{pp}(G)$
1.72	0.02	2.069	—	—	—	215.4
3.58	0.05	2.076	—	—	—	214.9
4.34	0.06	2.061	—	—	—	103.4
5.41	0.18	2.066	2.449	143.2	6.80	95.5
6.23	0.30 ^{b)}	2.062	2.452	145.8	7.17	92.8
9.19	>0.32 ^{b)}	2.059	2.454	148.5	7.69	92.7
~7 ^{c)}		2.063	2.26	174		

a) $G = (g_{\parallel} - 2) / (g_{\perp} - 2)$

b) Precipitation occurs

c) Copper-histidine complex covalently bonded on a silica matrix prepared by sol-gel method (data from [32])

nature of bonding between the metal ion and the donor atom. In this work, EPR spectra of the histidine-functionalized silica as a function of pH prepared in the presence of excess copper ion were measured at room temperature. Table 1 depicts EPR parameters for its copper complexes. The g values calculated from spectral data show that $g_{\parallel} > g_{\perp}$ which is characteristic of tetragonal or square planar geometry [29] and the value of $g_{\parallel} > 2.3$, indicates the ionic character of the metal-ligand bond [30]. If G value > 4.0 , then the local tetragonal axes are aligned parallel or only slightly misaligned; if $G < 4.0$, significant exchange coupling is present and the misalignment is appreciable [31]. In the histidine-functionalized silica the EPR spectra of copper ions adsorbed in media of pH greater than 5 revealed distinct differences from

those in media of pH less than 5. The copper-histidine functionalized silica complexes showed g_{\parallel} components in their EPR spectra. This was to be expected, since most of the imidazole groups in the histidine-functionalized silica exist in the free base form under these conditions. A greater extent of coordination would occur and a smaller motion of copper ions might be. Comparison of the EPR parameters with those of the copper-histidine complex covalently bonded on a silica matrix prepared by the sol-gel method [32], a ratio of copper to histidine residue equal to 2 was suggested. In other words, the CuN_4 model can be deduced from the complexing behavior of the histidine-functionalized silica.

The IR spectra of the histidine-functionalized silica and silica gel matrix were also measured. The functionalized silica exhibited peaks centered between 2800 and 3000 (C–H) and at 1644 (C=N), 1380 cm^{-1} (C=O). Neither of these features is observed on the silica support. Other potential features of the histidine spectrum such as -C–O, -C=O and -NH₂ bands are either too weak to be observed or are masked by the residual signals from the silica matrix and/or water adsorbed on the silica surface.

3.2 Analytical application of the histidine-functionalized silica

3.2.1 Packing procedure

Three kinds of home-made packed column were tested, as shown in Fig. 4. Basically, a retaining frit is made from silica and sodium silicate, and slurry of the stationary phase is pumped into the capillary at high pressure. Once packed, both retaining frits are burnt in place. The packed column coupled with an empty column having the detection window preinstalled in the instrument is then ready for use. Data presented typically represent an average of the results obtained on two separate columns. In this way, the column lifetime will be longer. Preliminary tests showed that the migration time of the first type of partially packed column exhibited serious variation. Both the first and the second type of packed columns required high voltage and a longer time for the injection (Figs. 4a and 4b). This might be due to a frit existing just adjacent the sample inlet end. Bubble formation easily arose while changing a new packed column. Meanwhile it was followed immediately by a breakdown in the current. For solving this problem, the third kind of packed column was adopted in all further experimental work (Fig. 4c). Due to the limitation of the capillary installation in Spectra PHOR-ESIS 100, a long open inlet length of capillary (at least 8 cm) has to be used. Of course, this will make the

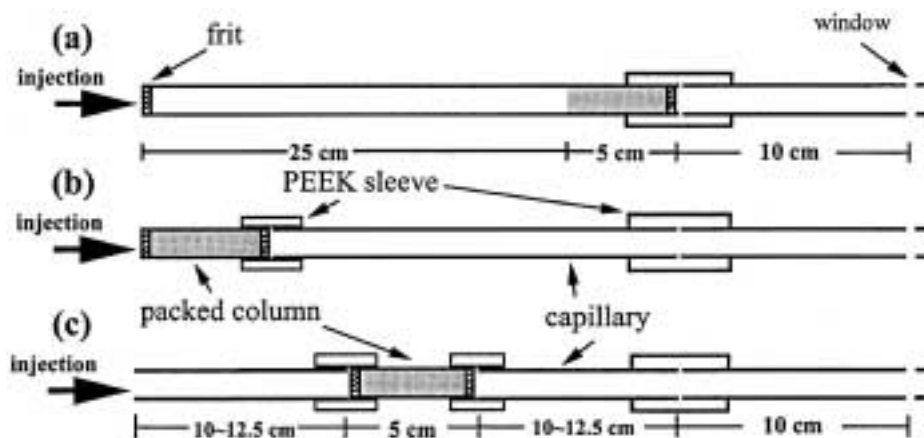


Figure 4. Three kinds of homemade packed column connected with a bare fused-silica capillary having the detection window preinstalled in the instrument. (a) A partially filled packed column as the separator. (b) A packed column coupled with a bare fused-silica capillary as the separator. (c) A packed column coupled with two pieces bare fused-silica capillary column as the separator.

assessment of the EOF more difficult. Therefore, the retention behavior was demonstrated with linear velocity in most cases.

3.2.2 Packing and frit stability

Observing the initial and average currents seems helpful for evaluating the properties of frit construction and stationary phase packing. If the initial current is zero, the following conditions might apply. (i) The column is not wholly occupied by the background electrolyte (BGE). (ii) The liquid level is too low in the buffer reservoir and no BGE can flow into the capillary. (iii) There is a blockage or a crack in the capillary. (iv) The concentration of BGE is too low. If a stable current cannot be achieved for a long time, this might be due to the following: (i) Bubble formation; (ii) contaminated BGE; (iii) a longer conditioning time is required. For a given system, the rate of heat generation is directly proportional to the molar conductivity of the solution (buffer type), the buffer concentration, the applied voltage squared and the column diameter squared and are inversely proportional to column length. Therefore, the current related to these parameters was also investigated.

3.2.2.1 Column length

When a potential difference is applied across a buffer-filled capillary, the presence of stationary phases would increase the resistance of the system. Resistance is inversely proportional to the current. With similar field strength (total length of 78 cm and applied voltage of -25 kV) and acetate buffer (10 mM, pH 5.0), the average current decreased as the histidine-functionalized silica packed column length increased (over the range of 5 ~ 40 cm

was tested). Bubble formation could be seen notably when a longer packed column was used. Twice the packed column length, from 20 to 40 cm, even a decrease of 70–80% current per unit length was observed, while under the above-mentioned condition but with phosphate buffer (10 mM, pH 5.0) and copper-histidine silica complex column, the current was merely changed from 5 to 3 μ A when the active bed length of 5 cm increased to 10 cm.

The mentioned behavior of the packed column (35 cm) compared also with that of a bare fused-silica capillary, having frits at both ends and similar column length. With the applied voltage of +20 kV and phosphate buffer (25 mM, pH 4.0), a stable current (35 μ A) displayed by coupling a buffer-filled capillary, while coupling an empty capillary column first then filling the buffer could see an unstable current with only 17 μ A initially then decreased gradually to 4 μ A after 5 min. Therefore, it can be concluded that coupling a buffer-filled capillary would be beneficial to the work. Additionally long time (40 min) was necessary for the migration of thiourea. The phenomenon may indicate that the surface chemistry of the frit might involve the retention of the solute more or less.

3.2.2.2 Type of buffer

Several kinds of buffer including acetic acid-sodium acetate, acetic acid-ammonium acetate, phosphoric acid-sodium dihydrogen phosphate and citric acid-sodium citrate have been tested as the BGE in this study. The results showed that at pH 4.0 no significant difference in current was observed except with citric acid. Since the equivalent conductivity [33] and the effective charge of citric acid at pH 4.0 are greatest among them (Table 2), the results are reasonable.

Table 2. Chemical and physical properties of the compounds related in this work

Compound	p <i>K</i> _a ^{a)} (25°C)	log <i>k</i> _f ^{b)}	Effective charge ^{c)}	Equiv. conduct. ^{d)}
Acetic acid (60) ^{e)}	4.75	1.83 ^{f)}	−0.166	40.9
Ammonium ion (18)	9.25	4.12 ^{g)}		
Phosphoric acid (98)	2.15; 7.20; 12.35	3.2 ^{f)}	−0.387	33; 33; 69
Citric acid (192.1)	3.13; 4.76; 6.40	5.90 ^{f)}	−1.025	70.2
Chloride (35.5)		−0.06 ^{g)}		76.35
Nitrite (46.0)		1.19 ^{g)}		71.80
Nitrate (62.0)		−0.01 ^{g)}		71.40
Sulfate (96.1)		0.95 ^{g)}		80.00
Benzoic acid (122.1)	4.20	1.76 ^{f)}	−0.387	32.4
Phthalic acid (166.1)	2.95; 5.40	2.69 ^{g)}	−0.956	52.3
Mandelic acid (152.2)	3.40	2.70 ^{g)}	−0.799	
Salicylic acid (138.1)	2.97	10.6 ^{f)}	−0.914	36.0
EDTA (292)	2.00; 2.66; 6.16; 10.24	18.80	−1.962	
Histidine (155.2)	1.82; 6.0; 9.2	10.16 ^{f)}	+1.00	

a) Data from [37, 38]

b) Formation constant of copper complex; data from [37–39]

c) Effective charge at pH 4.0

d) Limiting equivalent ionic conductance (S cm² equivalent^{−1}); data from [33]

e) Molecular mass

f) At 25°C, $\mu = 0.1$

g) At 25°C, $\mu = 1.0$

3.2.2.3 Buffer concentration

With the active bed length (5 cm), effective length (40 cm), total length (78 cm) and applied voltage of −20 kV increasing the citrate buffer concentration from 5 mM, 7.5 mM to 10 mM, the current increased from 3.5 μ A, 4 μ A to 4.5 μ A. It was found that a BGE concentration of more than 10 mM can give rise to Joule heating followed by loss of current as a result of bubble formation.

3.2.2.4 Applied voltage

The relationship between the current observed and the applied voltage was carried out under the condition of active bed length (10 cm), effective length (40 cm), total length (78 cm), and citrate buffer (10 mM, pH 4.0). The results demonstrated that −5 kV corresponded to 0.1 μ A, −10 kV to 1 μ A, −15 kV to 2 μ A, −20 kV to 3 μ A, and −25 kV to 4 μ A. With an applied voltage greater than −25 kV, a

deviation from the Ohm's law was indicated. Meanwhile this occurred along with bubble formation and was followed by the loss of current.

3.2.2.5 Organic modifier

Bubble formation may be easy to occur at low fraction of acetonitrile for CEC with hydrophobic stationary phase like octadecyl silica (ODS). Usually with the addition of acetonitrile a higher EOF velocity can be obtained because of its low viscosity. In this work, acetonitrile (5–10% v/v) has been tested as the mobile phase additive. Moreover, a smaller current and less EOF was found compared with that without the modifier. This might be due to the histidine-functionalized silica being a more hydrophilic stationary phase compared with ODS. For changing the linear velocity of the solute, other additives such as sodium dodecyl sulfate (SDS), cetyltrimethylammonium bromide (CTAB), and copper ion have been employed. As expected, CTAB may be adsorbed to the packing surface and increase the density of positive charge on the packing surface which results in higher EOF velocity. With a 20 cm histidine-functionalized silica active bed, 51 cm effective length, 83 cm total length, a mixture of phosphate buffer (pH 5.0, 25 mM) and CTAB (1 mM) as BGE, and the separation voltage of −25 kV, the migration time of mesityl oxide was 79 min. The calculated EOF is 3.57×10^{-5} cm²/Vs. Not only CTAB, but also SDS and copper ion, all increased the current to some extent compared with that without the modifier.

3.3 Column performance studies

When evaluating a new stationary phase, it is desirable to test both the EOF and the chromatographic performance. Several neutral markers were tested to give an indication of the EOF. Finally, the resolving power of the chromatographic phase was determined by the organic anions and inorganic anions. For the determination of EOF in CEC the choice of an appropriate neutral marker is not easy, since the neutral marker always has some interaction with the stationary phases [34]. Acetone, benzyl alcohol, dimethyl sulfoxide, mesityl oxide, and thiourea were selected as neutral markers for the histidine-functionalized silica and its copper complex packed columns. But all of them appeared to interact with the stationary phase. This resulted in a very small EOF and a rather long migration time.

With a copper-histidine functionalized silica complex active bed (10 cm), 51 cm effective length, 83 cm total length, phosphate buffer (pH 4.0, 25 mM), and a separation voltage of −20 kV, the migration time of thiourea was

190 min. From that, the calculated EOF was $1.86 \times 10^{-5} \text{ cm}^2/\text{Vs}$ (linear velocity, 0.27 cm/min). The linear velocity was measured using L_d/t , where L_d denotes the effective length of the capillary column and t is the elution time. With similar condition as that of the copper-histidine functionalized silica but with the applied voltage of +20 kV the EOF for the bare fused-silica having frits at both ends was $8.82 \times 10^{-5} \text{ cm}^2/\text{Vs}$ (40 min migration time; 1.28 cm/min linear velocity). A distinct lower EOF was demonstrated for the copper-histidine functionalized silica column.

3.3.1 Inorganic and organic ions

The most commonly used columns in CEC have been ODS columns, but in view of the need to maintain a high enough EOF and a hydrophobic surface of the stationary phase, ODS can only work well in a mobile phase with relatively high pH and the presence of an organic modifier. Therefore, there is an urgent need to develop new kinds of stationary phase suitable for CEC separation of strongly polar acidic compounds [35]. With histidine-functionalized silica and its copper complex, respectively, as the stationary phase, the effect of buffer pH on the linear velocity of potassium hydrogen phthalate (KHP) was studied. From Fig. 5 one can see that the linear velocity in the histidine-functionalized silica decreased dramatically over the pH range from 7 to 5. When KHP was run on the copper complex, no significant increase in analysis time on going from low to high pH was indicated. Results of this experiment may be rationalized that a smaller fraction of

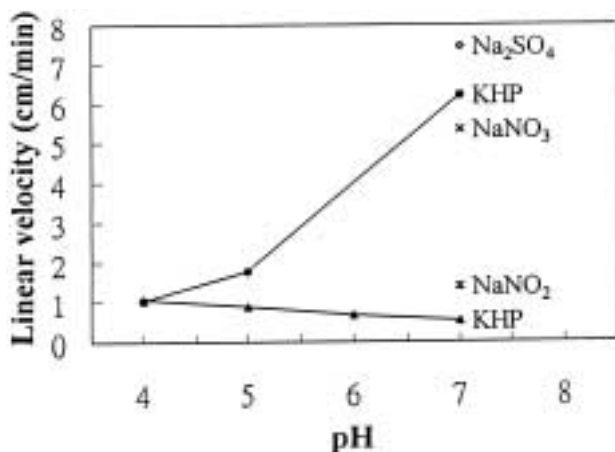


Figure 5. Effect of buffer pH on the linear velocity of potassium hydrogen phthalate. Capillary column, 100 μm ID packed with (●) histidine-functionalized silica (5 μm) or its copper complex (5 μm) (▲, ◇, ✱, ×), 10 cm packing length, 40 cm effective length, 78 cm total length; mobile phase, phosphate buffer (10 mM); sample concentration, 1 mM; electrokinetic injection: -2 kV, 2 s; separation voltage, -20 kV; detection, at 220 nm.

the protonated histidine-functionalized silica at higher pH values results in a less anion exchange reaction and this leads to a greater linear velocity. Besides, a larger electrophoretic mobility of the solute would be due to the greater fraction of the dissociated form, while for the copper-histidine complex increasing the pH results only in a slight decrease of linear velocity. This may reflect a more stable analyte-copper complex in the ligand exchange system. Moreover, at pH 4.0, there seems to be no significant difference in the linear velocity between these two stationary phases. In other words, the differences for the interaction force of the anion exchange and ligand exchange reactions might not be distinct.

With 10 cm active bed length of the copper-histidine complex, 40 cm effective length and 78 cm total length (100 μm ID) as well as phosphate buffer (pH 7.0, 10 mM) and a separation voltage of -20 kV, the linear velocities (cm/min) of NaNO_2 , NaNO_3 , Na_2SO_4 , and KHP were 1.36, 5.33, 7.43, and 0.49, respectively. Clearly the prepared CEC column is useful for the separation of all mentioned compounds, especially for nitrite and nitrate mixture, which is difficult in CE separation [36] due to the rather similar equivalent conductance (Table 2). In this work, the differences in linear velocity might be attributed to the greater coordinating property of nitrite ion toward the central copper ion than nitrate ion.

3.3.2 Separation of the test mixture

Phosphate and ammonium acetate buffer have been employed as the BGE for the separation of organic acid mixtures. However, retention times longer than 2 h were indicated. To shorten the analysis time, a shorter active bed (5 cm) and a stronger coordination buffer, which would interact with the central copper ion were used. As expected, sharp and symmetrical peaks were obtained in less than 12 min using citrate buffer (10 mM, pH 4.0) (Fig. 6A). The elution order is benzoic acid > D-mandelic acid > L-mandelic acid > KHP > salicylic acid. According to the effective charge and the stability constants of these compounds toward copper ion (Table 2), this fact strongly indicates that the separation mechanism is predominantly based on a ligand exchange reaction besides the electrophoretic mobility. Of course several other retention mechanisms might also be involved.

With lower concentration of citrate buffer (7.5 mM pH 4.0), five peaks can be observed but the elution strength decreased obviously (Fig. 6B). The elution time of the late-eluted salicylic acid is even more than 100 min with the citrate buffer (5 mM, pH 4.0) (data not shown). It can be seen that the retention decreased with increase of buffer concentration. The phenomena further prove that a dis-

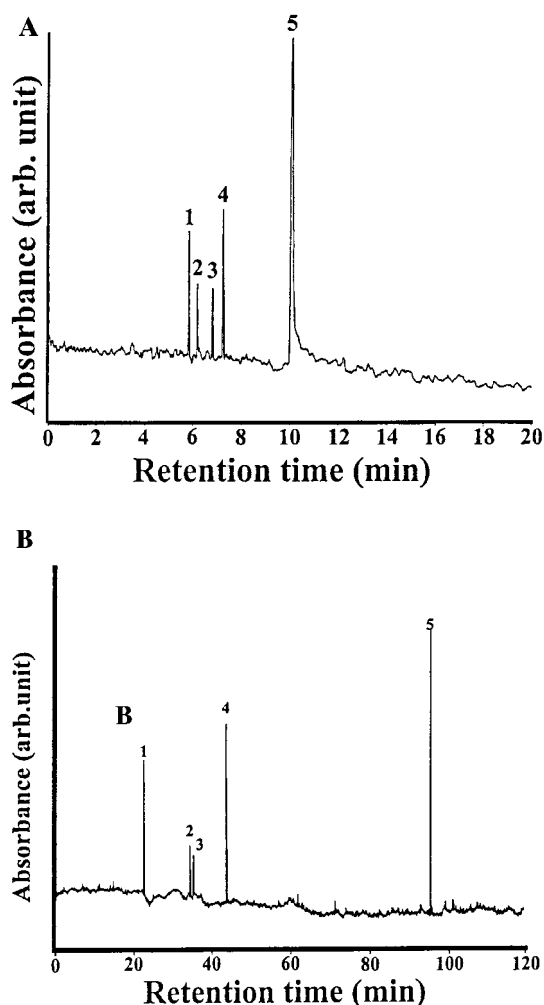


Figure 6. CEC separation of organic acids on copper-histidine functionalized silica with citrate buffer as mobile phase. Capillary column, 100 μm ID packed with copper-histidine functionalized silica (5 μm), 5 cm packing length, 35 cm effective length, 73 cm total length; sample concentration, 1 mM for each; electrokinetic injection, -2 kV, 2 s; separation voltage, -20 kV; detection, at 220 nm; mobile phase: (A) citrate buffer (10 mM, pH 4.0); (B) citrate buffer (7.5 mM, pH 4.0). Peak identification: 1, benzoic acid; 2, D-mandelic acid; 3, L-mandelic acid; 4, KHP; 5, salicylic acid.

placement reaction occurred. In other words, a ligand-exchange reaction indeed was involved in the separation mechanism. Additionally, the direction of EOF in bare fused-silica is opposite to that of the sample inlet. At lower ionic strength, the EOF may be more rapid resulting in slower migration of the solute to the packed column. Therefore, a longer time was needed for the elution of these solutes. Besides, the influence of the buffer concentration on the distinguishing ability of the enantiomer was found to be minor.

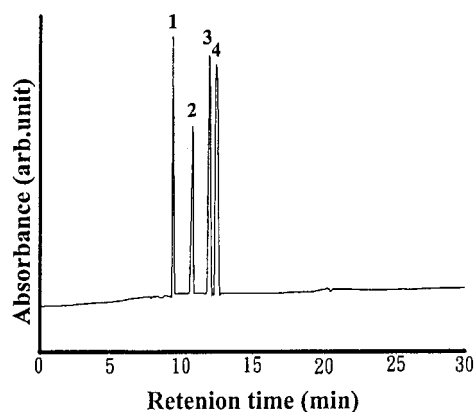


Figure 7. CEC separation of organic acids with EDTA buffer as mobile phase. Capillary column, 100 μm ID packed with copper-histidine functionalized silica (5 μm), 5 cm packing length, 40 cm effective length, 78 cm total length; sample concentration, 1 mM for each; electrokinetic injection, -2 kV, 2 s; separation voltage, -20 kV; detection at 220 nm; mobile phase, EDTA (5 mM, pH 4.0). Peak identification: 1, benzoic acid; 2, D- and L-mandelic acid; 3, KHP; 4, salicylic acid.

In order to understand the effect on retention behavior of a stronger chelating agent than citrate buffer, we chose EDTA (5 mM, pH 4.0) as the model. Not only less retention but also more complete elution, namely a greater peak area was observed (Fig. 7). Meanwhile the coelution of D- and L-mandelic acid was indicated. The predominant form of EDTA at pH 4.0 is H_2Y^{2-} . A greater effective charge and stronger coordinating ability (Table 2) results in the mentioned properties.

For the separation of organic acids, retention parameters and column performance summarized from Fig. 6A are listed in Table 3. The column efficiency for most of the analytes was more than 1.2×10^5 plates/m, except salicylic acid. However, columns were considered successfully made only if they were uniform and free of void after conditioning, use, and storage. Under the conditions of Fig. 6A, the relative standard deviations of the migration time are in the range of 3–7% for five consecutive injections. Of course reproducibility cannot be better as that of the open-tubular column. Improvements are expected by applying pressure to both ends of the capillary and frit more homogeneous.

4 Concluding remarks

On the basis of metal capacity and EPR studies, it was shown that the prepared histidine-functionalized silica forms a $\text{Cu}(\text{histidine})_2$ complex. Both histidine-functionalized silica and the copper-histidine complex were

Table 3. Separation efficiency of the copper-histidine functionalized silica complex in packed CEC^{a)}

Analyte	Retention time (min)	Peak width (min)	Half peak width (min)	Plate height (μm)	$N^{\text{b)}$ (plates m^{-1})	$R_s^{\text{c)}$
Benzoic acid	5.828	0.057	0.035	0.322 (0.064) ^{d)}	153 600	–
D-Mandelic acid	6.180	0.056	0.033	0.261 (0.052)	194 290	6.23
L-Mandelic acid	6.816	0.072	0.046	0.404 (0.081)	121 630	9.94
KHP	7.252	0.078	0.049	0.418 (0.083)	121 350	5.81
Salicylic acid	10.103	0.189	0.117	1.200 (0.240)	41 310	21.36

a) Capillary column; 100 μm ID, 5 cm packing length with 5 μm copper-histidine functionalized silica complex, 35 cm effective length, 73 cm total length; background electrolyte, citrate (10 mM, pH 4.0); sample concentration; 1 mM for each, electrokinetic injection; –2 kV for 2 s; separation voltage, –20 kV; detection, at 220 nm

b) Plate numbers

c) Resolution

d) Reduced plate height

employed as stationary phases of a CEC-packed column. Experimental conditions are simple and well controlled with the packed column coupled with an empty column having the detection window preinstalled in the instrument. Due to the frit not being made just adjacent to the end of sample inlet, bubble formation was suppressed and a shorter injection time and a lower injection voltage were needed. Among parameters, which affect the electrical current, we found that the packed column length and the applied voltage are the predominant factors. Of course, other factors such as buffer type, pH, concentration, and type of organic modifier also affect the current. Several mechanisms including electrophoretic migration, ion exchange, and hydrophobic interactions are involved in the separation of the test mixture. However, in the histidine-functionalized silica packed column, ion exchange seems to be the predominant reaction, while in the copper-histidine complex packed column, the ligand-exchange reaction seems to predominate. These findings demonstrate that the stationary phases are highly promising. Columns of virtually any length are easily accessible. This flexibility enables the easy tailoring of both the interactions that are required for specific modes as well as the level of EOF generated by the support. More detailed investigations are still necessary for the applicability to other electron-donating compounds. Better reproducibility could be expected if homogeneous frits and additional pressure facilities at the capillary ends are available.

The authors thank the National Science Council of Taiwan for financial support.

Received February 13, 2001

5 References

- [1] Palm, A., Novotny, M. V., *Anal. Chem.* 1997, **69**, 4499–4507.
- [2] Chen, J. R., Dulay, M. T., Zare, R. N., Svec, F., Peters, E., *Anal. Chem.* 2000, **72**, 1224–1227.
- [3] Kelly, K. A., Khaledi, M. G., in: Khaledi, M. G. (Ed.), *High Performance Capillary Electrophoresis*, Wiley, New York 1998, Chapter 8.
- [4] Pesek, J. J., Matyska, M. T., *Electrophoresis* 1997, **18**, 2228–2238.
- [5] Colon, L. A., Maloney, T. D., Fermier, A. M., *J. Chromatogr. A* 2000, **887**, 43–53.
- [6] Pursch, M., Sander, L. C., *J. Chromatogr. A* 2000, **887**, 313–326.
- [7] Liu, C. Y., *Electrophoresis* 2001, **22**, 612–628.
- [8] Smith, N. W., Evans, M. B., *Chromatographia* 1995, **41**, 197–203.
- [9] Altria, K. D., Smith, N. W., Turnbull, C. H., *J. Chromatogr. B* 1998, **717**, 341–353.
- [10] Carney, R. A., Robson, M. M., Bartle, K. D., Mayers, P., *J. High Resolut. Chromatogr.* 1999, **22**, 29–32.
- [11] Cikalo, M. G., Bartle, K. D., Mayers, P., *Anal. Chem.* 1999, **71**, 1820–1825.
- [12] Ye, M., Zou, H., Liu, Z., Ni, J., *J. Chromatogr. A* 2000, **887**, 223–231.
- [13] Lämmerhofer, M., Tobler, E., Lindner, W., *J. Chromatogr. A* 2000, **887**, 421–437.
- [14] Koide, T., Ueno, K., *J. High Resolut. Chromatogr.* 2000, **23**, 59–66.
- [15] Kitagawa, S., Tsuda, T., *Anal. Sci.* 1998, **14**, 571–575.
- [16] Zhang, M., El Rassi, Z., *Electrophoresis* 1998, **19**, 2068–2072.
- [17] Zhang, M. Q., El Rassi, Z., *Electrophoresis* 1999, **20**, 31–36.
- [18] Huang, P., Jin, X., Chen, Y., Srinivasan, J. R., Lubman, D. M., *Anal. Chem.* 1999, **71**, 1786–1791.
- [19] Zhang, M., Ostrander, G. K., El Rassi, Z., *J. Chromatogr. A* 2000, **887**, 287–297.
- [20] Spikmans, V., Lane, S. J., Smith, N. W., *Chromatographia* 2000, **51**, 18–24.
- [21] Ye, M., Zou, H., Liu, Z., Ni, J., Zhang, Y., *Anal. Chem.* 2000, **72**, 616–621.

- [22] Klampfl, C. W., Hilder, E. F., Haddad, P. R., *J. Chromatogr. A* 2000, **888**, 267–274.
- [23] Liu, C. Y., *Anal. Chim Acta* 1987, **192**, 85–93.
- [24] Nesterenko, P. N., Ivanov, A. V., *J. Chromatogr. A* 1994, **671**, 95–99.
- [25] Hajos, P., *J. Chromatogr. A* 1997, **789**, 141–148.
- [26] Macka, M., Haddad, P. R., *J. Chromatogr. A* 2000, **884**, 287–296.
- [27] Yamamoto, H., Baumann, J., Erni, F., *J. Chromatogr.* 1992, **593**, 313–319.
- [28] Liu, C. Y., Chen, M. J., Lee, N. M., Hwang, H. C., Jou, S. T., Hsu, J. C., *Polyhedron* 1992, **11**, 551–558.
- [29] Ballhausen, C. J., *Introduction to Ligand Field Theory*, McGraw-Hill, New York 1962, p. 134.
- [30] Kivelson, D., Neiman, R., *J. Chem. Phys.* 1961, **35**, 149–155.
- [31] Hathaway, B. J., Billing, D. E., *Coord. Chem. Rev.* 1970, **5**, 143–207.
- [32] Louloudi, M., Deligiannakis, Y., Hadjiliadis, N., *Inorg. Chem.* 1998, **37**, 6847–6851.
- [33] Dean, J. A., *Lange's Handbook of Chemistry*, McGraw-Hill, New York 1985.
- [34] Lelievre, F., Yan, C., Zare, R. N., Gareil, P., *J. Chromatogr. A* 1996, **723**, 145–156.
- [35] Zhang, L., Zhang, Y., Shi, W., Zou, H., *J. High Resol. Chromatogr.* 1999, **22**, 666–670.
- [36] Takayanagi, T., Wada, E., Motomizu, S., *Anal. Sci.* 1996, **12**, 575–579.
- [37] Martell, A. E., Smith, R. M., *Critical Stability Constants*, Plenum Press, New York 1982, Vol. 5, p. 336.
- [38] Smith, R. M., Martell, A. E., *Critical Stability Constants*, Plenum Press, New York 1989, Vol. 6, pp. 32, 306, 315, 338.
- [39] Smith, R. M., Martell, A. E., *Critical Stability Constants*, Plenum Press, New York 1976, Vol. 4, pp. 47, 50.